Chapter 8
Model Container Design for Soil-Structure Interaction Studies

Subhamoy Bhattacharya, Domenico Lombardi, Luiza Dihoru, Matt S. Dietz, Adam J. Crewe, and Colin A. Taylor

Abstract Physical modelling of scaled models is an established method for understanding failure mechanisms and verifying design hypothesis in earthquake geotechnical engineering practice. One of the requirements of physical modelling for these classes of problems is the replication of semi-infinite extent of the ground in a finite dimension model soil container. This chapter is aimed at summarizing the requirements for a model container for carrying out seismic soil-structure interactions (SSI) at 1-g (shaking table) and N-g (geotechnical centrifuge at N times earth's gravity). A literature review has identified six types of soil container which are summarised and critically reviewed herein. The specialised modelling techniques entailed by the application of these containers are also discussed.

8.1 Introduction

8.1.1 Physical Modelling in Earthquake Engineering

The structural failures and loss of life in recent earthquakes have shown the shortcomings of current design methodologies and construction practices. Post earthquake reconnaissance investigations have led to improvements in engineering

S. Bhattacharya (✉) • D. Lombardi • L. Dihoru • M.S. Dietz • A.J. Crewe • C.A. Taylor
Department of Civil Engineering, University of Bristol, Queen's Building,
University Walk, Bristol BS8 1TR, UK
e-mail: s.bhattacharya@bristol.ac.uk; domenico.lombardi@bristol.ac.uk;
Luiza.Dihoru@bristol.ac.uk; M.Dietz@bristol.ac.uk; a.j.crewe@bristol.ac.uk;
colin.taylor@bristol.ac.uk

Table 8.1 Historical development of earthquake engineering practice after Bhattacharya et al. (2011a)

Earthquake	Remarks	Post earthquake developments
28th Dec, 1908 Reggio Messina earthquake (Italy)	120,000 fatalities. A committee of nine practising engineers and five professors were appointed by Italian government to study the failures and to set design guidelines	Base shear equation evolved, i.e. the lateral force exerted on the structure is some percentage of the dead weight of the structure (typically 5–15%)
1923 Kanto earthquake (Japan)	Destruction of bridges, buildings. Foundations settled, tilted and moved	Seismic coefficient method (equivalent static force method using a seismic coefficient of 0.1–0.3) was first incorporated in design of highway bridges in Japan (MI 1927)
10th March, 1933 Long Beach earthquake (USA)	Destruction of buildings, especially school buildings	UBC (1927) revised. This is the first earthquake for which acceleration records were obtained from the recently developed strong motion accelerograph
1964 Niigata earthquake (Japan)	Soil can also be a major contributor of damage	Soil liquefaction studies started
1971 San Fernando earthquake (USA)	Bridges collapsed, dams failed causing flood. Soil effects observed	Liquefaction studies intensified. Bridge retrofit studies started
1994 Northridge earthquake (USA)	Steel connections failed in bridges	Importance of ductility in construction realised
1995 Kobe earthquake (Japan)	Massive foundation failure. Soil effects were the main cause of failure	Downward movement of a slope (lateral spreading) is said to be one of the main causes. JRA (1996) code modified (based on lateral spreading mechanism) for design of bridges

analysis, design and construction practices. A brief historical development of earthquake engineering practice illustrating how earthquake engineers have learned from failures in the past is outlined in Table 8.1. Therefore, before applying any earthquake resistant design method to practical problems, or establishing a proposed failure mechanism, it is better to seek verification from all possible angles. Obtaining data from physical systems (i.e. physical modelling) on the performance of the design method is essential to that verification. Such data ideally could be acquired from detailed case histories during earthquakes but only by putting society at risk in the meantime. The fact that large earthquakes are infrequent and that most structures are not instrumented makes this method of verification difficult. Alternatively, a record of observations of the response of a physical system can be acquired by modelling.

Fig. 8.1 Damage predominantly due to structural inadequacies observed during the 2001 Bhuj earthquake

Fig. 8.2 Collapse of Bio-Bio Bridge during the 2010 Chile earthquake

8.1.2   Seismic Soil-Structure Interaction Problems

Structural failure during earthquakes can result from inadequacies of either the structure itself, its foundation, or a combination of both. Figure 8.1 shows the failure of a residential building predominantly due to structural inadequacies such as poor ductility and improper beam-column detailing. On the other hand, the failures shown in Fig. 8.2 are probably due to foundation failure or soil-structure interaction. In such failures the soil supporting the foundation plays an important role. The behaviour of foundations during earthquakes is often dictated by the response of the supporting soil. In general, there are two problematic types of ground response: (a) liquefaction, such as seen in the 1995 Kobe earthquake; (b) amplification of the ground motion, such as seen during the 1989 Loma Prieta earthquake in California or the 1985 Mexico earthquake.

Fig. 8.3 Kandla port building

8.1.3 Physical Modelling of Seismic-Soil Structure Interaction Problems

Figure 8.3 shows a piled building in Kandla, which tilted towards the Arabian Sea during the 2001 Bhuj (India) earthquake. The operative mechanism that enabled the tilting is hidden and since earthquakes are very rapid events and as much of the damage to piles occurs beneath the ground, it is hard to ascertain the failure mechanism without undertaking a costly excavation. Alternatively, physical modelling can be used to gain an understanding of the operative mechanisms.

8.1.4 Structure of the Chapter

The chapter is structured in the following way. Section 8.2 presents the two types of geotechnical seismic testing carried out: shaking table test at 1-g and geotechnical centrifuge testing. Some modelling issues are also discussed. Section 8.3 develops the requirements of a model soil container from first principles which are valid at 1-g (shaking table) or N-g testing (centrifuge). Section 8.4 of the chapter critically reviews the six different types of model container used for testing.

8.2 Physical Modelling

8.2.1 1-g Model Tests Using Shaking Table

The behaviour of soil is non-linear and stress dependent. Soils that show contractive behaviour (loose to medium dense sand) under high normal stress may exhibit a dilative behaviour at low stress level. Therefore, physical modelling of geotechnical problems should ensure that stress dependent behaviour is correctly accounted for. High gravitational stresses cannot be produced in a shaking table test. The typical height of soil container varies between 0.5 and 6.3 m and therefore the vertical effective stress is limited to a maximum of 5 kPa (saturated sand) to about 120 kPa (dry sand). The effect of stress dependency on soil strength dominated problems (for example slope failure) in 1-g testing can be addressed through the change in soil density in model ground. It must be mentioned that in some dynamic soil-structure-interaction problems stiffness rather than strength governs and this issue is dealt in the subsequent paragraphs.

In shallow soil container, the isotropic stress level controlling the mechanisms under investigation is low, leading to higher friction angle but at the same time low shear modulus when compared to its equivalent prototype. Many researchers, such as Kelly et al. (2006), Leblanc et al. (2010), address the issue by pouring the sand at lower relative density. Figure 8.4 shows the variation of the peak friction angle (φ')
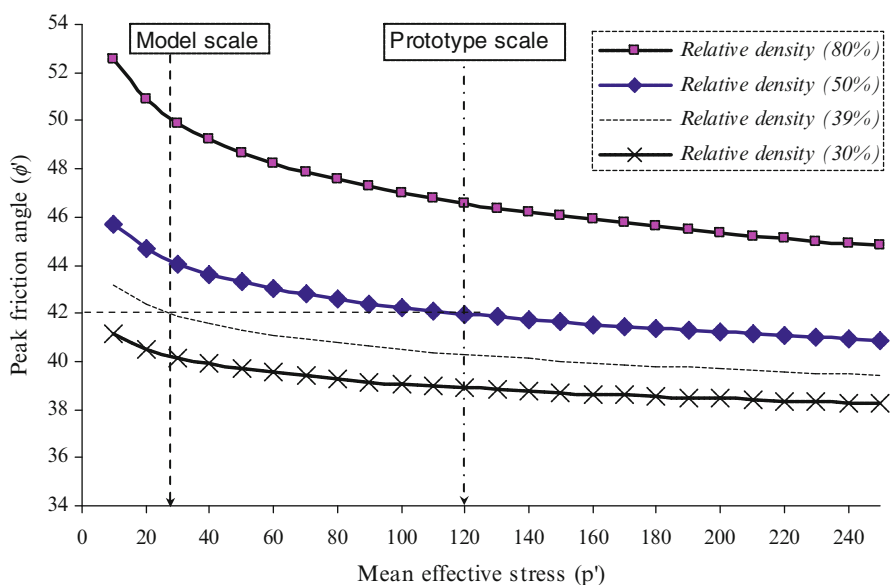

Fig. 8.4 Friction angle of Leighton Buzzard Sand as a function of mean effective stress and relative density

with mean effective isotropic stress (p') for silica sand having various relative density based on Eq. 8.1 following the stress-dilatancy work of Bolton (1986).

$$\phi' = \phi_{cv} + 3\left[R_D\left(9.9 - \ln p'\right) - 1\right]$$

(8.1)

where:

R_D = Relative density of the sand
ϕ_{cv} = Critical State Angle of Friction of the sand; it is 34.3° for Leighton Buzzard sand
p' = Isotropic stress in kPa

Based on this approach, if 120 kPa of mean effective prototype stress at 50% relative density is to be modelled in a small scale laboratory model at 25 kPa stress, the sand is to be poured at about 39% relative density ensuring that the peak friction angle is the same. There is limitation in this approach in the sense that there is a minimum density beyond which sand cannot be poured and other secondary effects become important.

While the effect of peak friction angle in 1-g testing can be resolved using the method presented in Fig. 8.4, further thought is required to address the issue of shear modulus, G. The shear modulus of a soil is function of effective stress shown by Eq. 8.2.

$$G \propto p'^n$$

(8.2)

where the value of n depends on the type of soil. The value of n varies between 0.435 and 0.765 for sandy soil (Wroth et al. 1979) but a value of 0.5 is commonly used. For clayey soil, the value of n is generally taken as 1.

While deriving the scaling laws or non-dimensional groups for a physical model the above concepts should be taken into consideration. These are necessary to interpret the model test results in order to scale up the results for prediction of prototype consequences. Every physical process can be expressed in terms of non-dimensional groups and the fundamental aspects of physics must be preserved in the design of model tests. The necessary steps associated with designing such a model, to be implemented either in 1-g or a multi-g testing (centrifuge) environment, can be stated as follows:

1. To deduce the relevant non-dimensional groups by thinking of the mechanisms that govern the particular behaviour of interest both at model and prototype scale.
2. To ensure that a set of scaling laws are simultaneously conserved between model and prototype through pertinent similitude relationships.
3. To identify scaling laws which are approximately satisfied and those which are violated and which therefore require special consideration.

While deriving the non-dimensional groups, appropriate soil stiffness should be taken into consideration. Examples of derivation of scaling laws for general dynamic problems can be found in the literature, see for example Iai (1989), Muir Wood et al. (2002), Bhattacharya et al. (2011b).
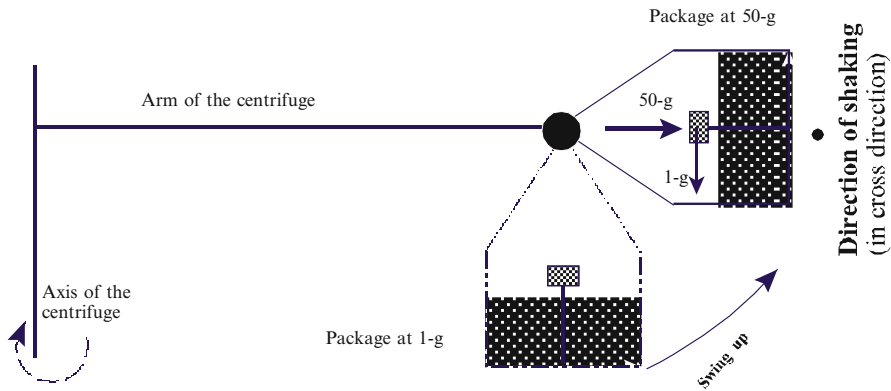
Fig. 8.5   Schematic diagram showing the working principle of a geotechnical centrifuge

8.2.2   Dynamic Geotechnical Centrifuge Tests

An alternative way of modelling is through the use of a geotechnical centrifuge which enables the recreation of the same stress and strain level within the scaled model by testing a 1:N scale model at N times earth's gravity, created by centrifugal force (see Fig. 8.5). In the centrifuge, the linear dimensions are modelled by a factor 1/N and the stress is modelled by a factor of unity. Scaling laws for many parameters in the model can be obtained by simple dimensional analysis, and are discussed by Schofield (1980 and 1981).

8.3   Requirements of a Model Container

Soil strata within the ground or underneath a prototype structure have infinite lateral extent while a model test will have a finite size. The challenge is therefore to replicate the boundary conditions of a ground in a container with finite dimensions. Figure 8.6 shows the pattern of soil deformation along the soil layers. The theoretical pattern of deformation is dependent on the assumption one makes regarding the variation of shear modulus with depth. It may be noted that the displacement is constant at a particular horizontal plane and the amplitude of displacement varies with depth. The soil column can therefore be idealised as a shear beam. Figure 8.7 shows the comparison of a shear beam with Euler-Bernoulli beam. The design of the soil container should be carried out in such a way to replicate as close as practicable the stress-strain condition of an infinite lateral extent and finite depth soil profile, when subjected to a 1-dimensional horizontal shaking, see Fig. 8.6.
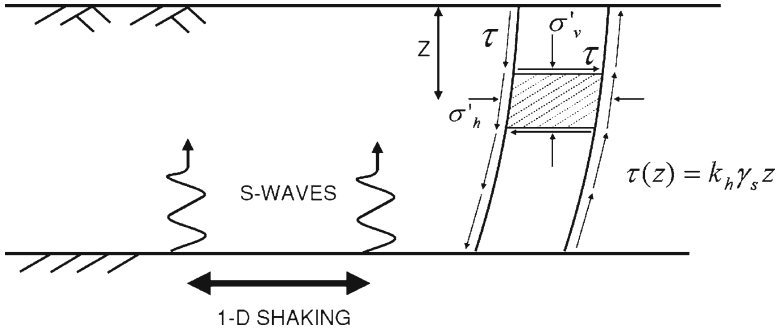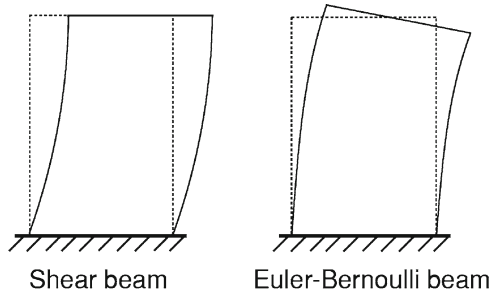
Fig. 8.6 Soil layer of infinite lateral extent and finite depth subjected to a base shaking at its bedrock

Fig. 8.7 Shear beam and Euler-Bernoulli beam

Shear beam   Euler-Bernoulli beam

8.3.1   Before Shaking (Geostatic Condition)

The stress field at any point in a given plane in a mass of the soil can be represented by normal and shear stresses. The effective vertical and horizontal stresses are given by:

$$\sigma'_v = \gamma z \tag{8.3}$$

$$\sigma'_h = K_0 \sigma'_v \tag{8.4}$$

Where γ and K_0 are the unit weight of the soil and the coefficient of lateral earth pressure at rest respectively.

In the geostatic condition the vertical and horizontal planes are principal stress planes and the normal stresses acting on them are principal stresses. The vertical and horizontal stresses are also principal stresses as can also be deduced from the pole (*P1*) of the Mohr circle illustrated in Fig. 8.8.
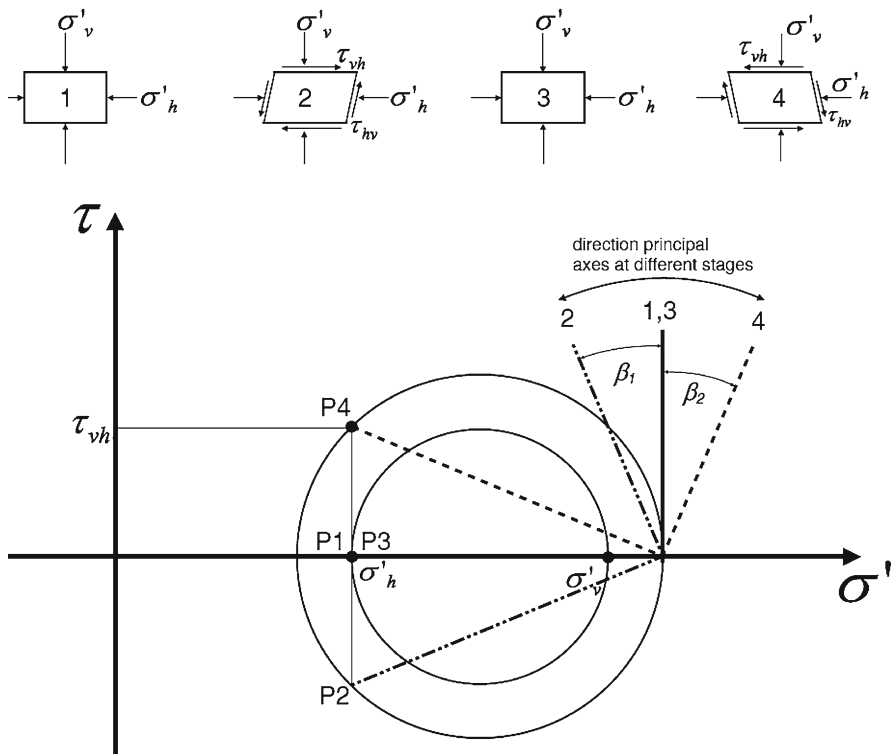
Fig. 8.8 Stress path of a soil element when subjected to horizontal shaking (Adapted from Kramer (1996))

8.3.2   *During Shaking*

As the horizontal shaking starts, shear waves (indicated by S-waves in Fig. 8.6) propagate vertically upward within the soil. Normal stresses remain constant while shear stresses in both vertical and horizontal planes increases. The shear stress induced by the horizontal shaking may be estimated by Eq. 8.5.

$$\tau(z) = k_h \gamma z \tag{8.5}$$

where k_h represents the coefficient of horizontal acceleration. The stress field induced by the shaking causes a rotation of the vertical planes while the horizontal planes remain horizontal. This state of stress is also shown in Mohr circle (Fig. 8.8). Since the horizontal and vertical stresses are constant, the Mohr circle increases in size while its centre remains unchanged. Therefore the principal axes will rotate (anticlockwise in this case) and the new position of the pole is now indicated by *P2* (Fig. 8.8). Taking into account the cyclic nature of the shear stresses the principle axes will continuously change denoted by angle *β*.
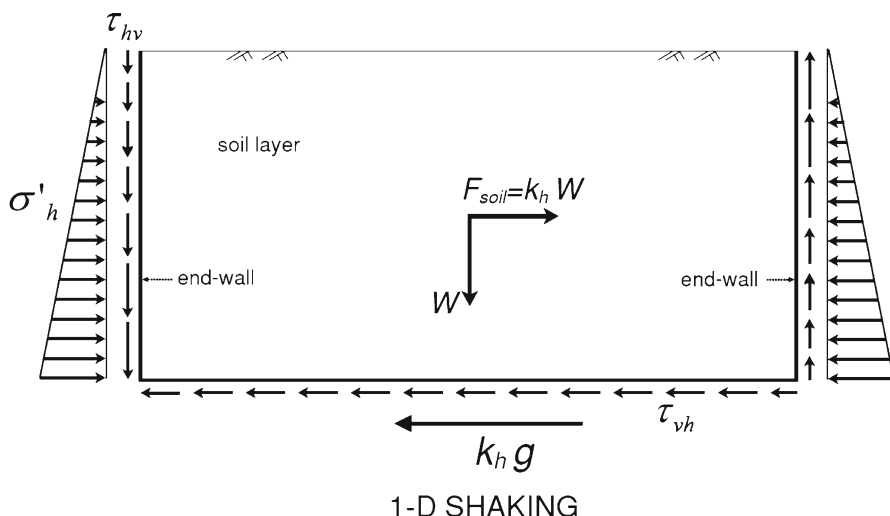
Fig. 8.9 Schematic representations of shear and normal stresses generated within the soil layer due to the inertia of the soil (Adapted from Zeng and Schofield (1996))

8.3.3 Stress Similarity

The horizontal shaking generates shear stresses in both vertical and horizontal planes. If the container end walls are frictionless, vertical stresses cannot develop and the stress field near the boundaries will be different from that of the prototype. However, if the model is tested in the central part of the box at a considerably large distance from the end-walls, such effects can be assumed to be minimal. The evaluation of the distance beyond which the stress field is not affected by the boundaries is complex and requires detailed experimental or numerical analysis. During shaking, the mass of the soil generates an inertia force that can be considered as a horizontal load given by Eq. 8.6 and acts at the centre of inertia of the soil layer (see Fig. 8.9)

$$F_{soil} = k_h W \tag{8.6}$$

Figure 8.9 shows that (for the particular case considered here) the inertia force of the soil generates a clockwise overturning moment. For the stability of the system this overturning moment must be balanced by the shear stresses acting on the vertical plane. Therefore in absence of adequate friction between the end-walls and the adjacent soil, the shear stresses may not be capable of balancing the overturning moment.

8.3.4 Propagation of the Shaking to the Soil Layer

An important feature of the soil container is represented by the fact that the shaking applied to the base of the container should be transferred to the upper layer of the soil.

This condition can be accomplished by the use of a rough base, which enables the generation of shear stresses in the horizontal plane (i.e. at the interface between the soil and the base of the container).

8.3.5 Strain Similarity

The displacement profile of the soil induced by the shaking has to satisfy the condition that at a particular depth the displacement is constant. In other words, the horizontal cross section must remain horizontal. In the model container, the finite dimension of its width (the dimension orthogonal to the shaking) may cause an alteration of the plane-strain conditions. This may be avoided by making the side walls smooth for 1-dimensional shaking tests.

8.3.6 P-Waves Generation and Reflection Problems

S-waves will propagate through the soil layer (see Fig. 8.6). However, during shaking, the soil next to the boundaries may undergo under compression and extension and P-waves may be generated. Therefore the response of the model will be affected by the interaction between P and S waves. Another consideration that must be taken into account is therefore the reflection of the waves from the artificial boundaries. In an infinitely extended soil layer this phenomenon is absent since there are no boundaries and the energy of the waves diminishes with distance. The attenuation of the energy may be explained considering two different mechanisms: The first mechanism is the friction generated by the sliding of the grain particles which converts part of the elastic energy to heat. This dissipation may be considered as function of the hysteretic damping of the soil. The second mechanism is due to the radiation damping which is related to the geometry of the propagation of the waves. As waves propagate, their energy will spread to a greater volume of soils and this is also known as geometric attenuation which can occur even in absence of damping. Further details can be found in Kramer (1996).

8.3.7 Water Tightness

If the tests are carried out in saturated soils, the soil container must be watertight.
In summary, a model container has to satisfy the following criteria:

1. Maintain stress and strain similarity in the model as in the prototype
2. Propagate the base shaking to the upper soil layers
3. Reduce the wave reflections (energy) from the sidewalls which would otherwise radiate away in the prototype problem. Also to ensure negligible P-waves generation due to the presence of artificial boundary.

4. For saturated soil tests (i.e. liquefaction tests), the soil container should be watertight.

   Some additional conditions need to be satisfied:

1. The model container must have adequate lateral stiffness so that a zero lateral strain (K_0 condition) condition can be maintained. This is particularly pronounced in centrifuge testing during the centrifuge spin-up.
2. The frictional end walls must have the same vertical settlement as the soil layer so that no additional stresses are induced in the soil. This effect is particularly important in centrifuge testing during the swing up. However, in 1-g testing any unwanted component of vertical motion should not induce additional stress in the soil at the boundaries.

   Further details on the conditions related to the centrifuge testing can be found in Brennan (2003), Zeng and Schofield (1996).

8.4   Different Types of Container

The design requirements illustrated in the previous section can be achieved through various types of container design. It must be mentioned however that each of the designs has its own advantages and disadvantages, and they satisfy the different design requirements to a different degree. The different types of soil container available can be summarised as follow:

1. Rigid container
2. Rigid container with flexible boundaries (e.g. duxseal or sponge)
3. Rigid container with hinged end-walls
4. Equivalent Shear Beam (ESB) container
5. Laminar container
6. Active boundary container

8.4.1   Rigid Container

Figure 8.10 shows a schematic diagram of a rigid box. In this design, the shear stiffness of the end walls is much higher than the stiffness of the layers of soil contained by it. The end walls and the base of the container are also designed to be rough which is achieved by gluing a layer of sand onto it. This ensures the development of shear stresses in vertical plane at the interface between the container and soil. As discussed in the previous section, the rough base enables the base shaking to propagate through the soil layer. In order to maintain the plane strain condition, the surfaces of the side-walls must be very smooth which is often accomplished by treating the
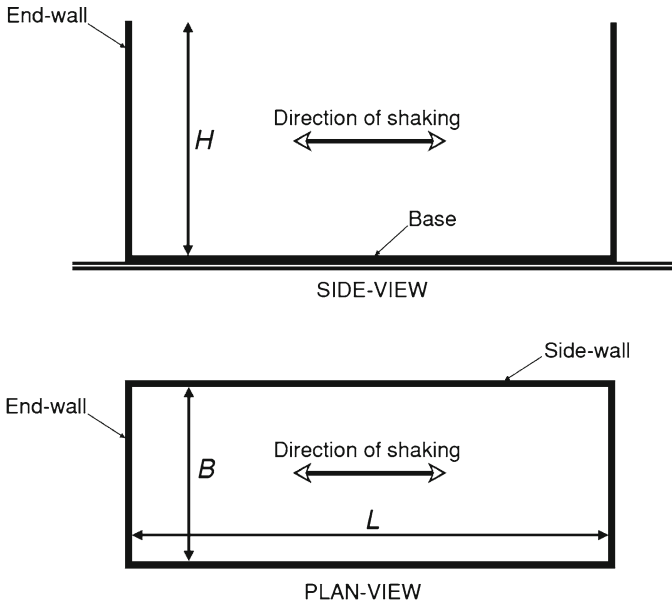
Fig. 8.10 Schematic diagram of a rigid container

inner surfaces of the container with grease or oil or by a plastic material (e.g. teflon or latex). An alternative design that achieves a similar effect uses smooth glass as the side-walls.

An important issue that has to be taken into account during the design is the ratio between the length and the height of the container. Numerical studied conducted by Fishman et al. (1995) and Whitman and Lambe (1986) quantified the zones close to the end walls that are affected by the artificial boundary. Their study suggests that this zone extends from the end walls into the container a distance of up to 1.5–2.0 times the height of the container. Based on these considerations, it may be suggested that the ratio of the length, L, of the container to the height, H, (see Fig. 8.10 for the notation of the symbols) should be more than 4. Table 8.2 lists several examples of rigid soil container founded in the literature.

8.4.2 Rigid Container with Flexible Boundary

In order to limit the reflection of the waves from the rigid boundary (one of the limitations of a rigid container) some adjustments can be made. Essentially the end-wall conditions are modified by the use of soft materials such as *sponge* that are glued along the end-walls of the container (see Fig. 8.12). The benefits are the following: (a) a partial reduction of the reflection of the waves, (b) reduction of the lateral

Table 8.2 Example of rigid containers presented in the literature

| Shape	Shaking direction	L-B-H [mm]	L/H	Side-walls	Base & end-walls	Testing	Reference
Rectangular	1-D	597-270-150	4.0	Teflon	Rough sand paper	Centrifuge	Adalier and Elgamal (2002)
Rectangular	1-D	500-565-190	2.6	No-details	No-details	Centrifuge	Whitman and Lambe (1986)
Rectangular (Fig. 8.11a)	2-D	712-432-440	1.6	Smooth plastic membrane	Base covered by sand-glue mixture.	Centrifuge	Ng et al. (2004)
Rectangular (Fig. 8.11c)	1-D	1,500-400-1,000	1.5	Perspex and wood plates	Terram geotextile membrane	Shaking table	Norton (2008)
Rectangular (Fig. 8.11b)	1-D	450-240-400	1.1	Perspex	PTFE (poly-tetra-fluoro-ethylene) sheets	Shaking table	Dash (2010)
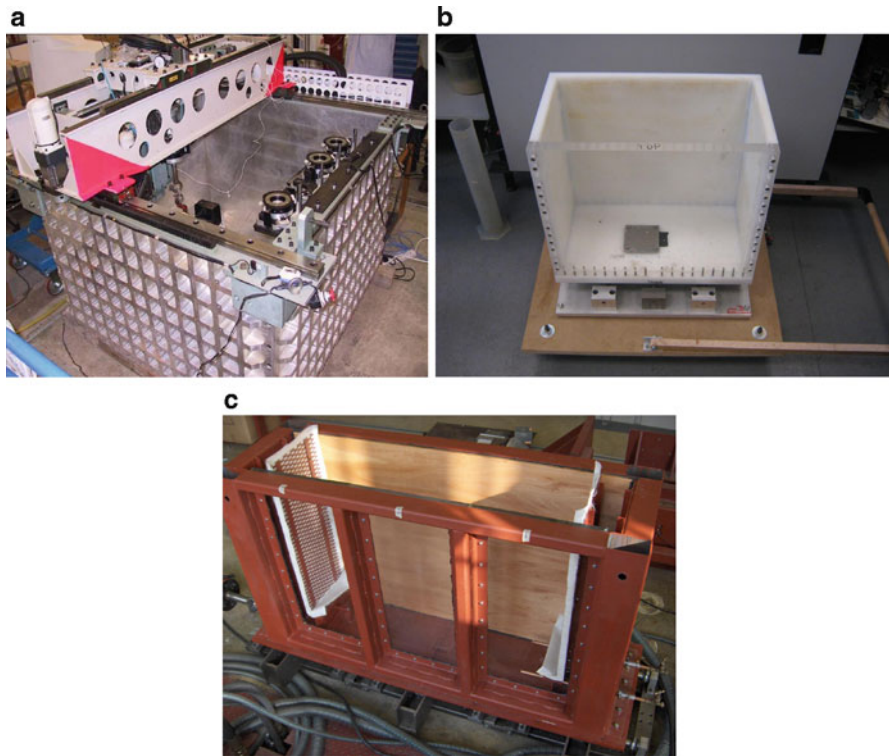
Fig. 8.11 Examples of rigid container: (**a**) Rigid container used in centrifuge at the Hong Kong University of Science and Technology (HKUST) (Courtesy of Prof Charles W.W. Ng). (**b**) Rigid box used in the small shaking table at the University of Bristol. (**c**) Rigid box used in the shaking table at the University of Oxford
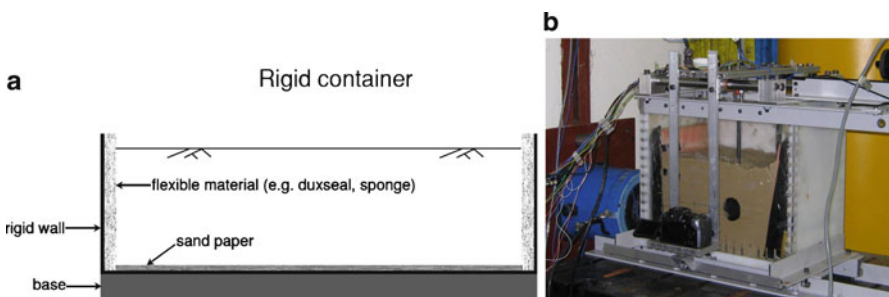

Fig. 8.12 Rigid container with flexible boundaries: (**a**) Schematic diagram (**b**) Example used in the Bristol Laboratory for Advanced Dynamics Engineering (BLADE)

stiffness of the end wall. The effect of sponge on K_0 condition is not yet established and needs further research. A pipe sealant material such as Duxseal has been used in the centrifuge modelling. Cheney et al. (1988) and Steedman and Madabhushi (1991) suggested that a third of the incident waves are reflected by the duxseal

boundaries. It must be mentioned that duxseal material being much stiffer than normal sponge is recommended for centrifuge applications. However, the application of softer materials at the end-walls of the soil container raises some uncertainties regarding the actual boundary conditions. Moreover, the reflection of the waves is not completely eliminated. Table 8.3 lists some examples of rigid container with flexible boundaries.

8.4.2.1 Advantages

The main advantage of this type of design when compared with a rigid box is the reduction of the wave reflection and the P-wave generation.

8.4.2.2 Limitations

There are two main limitations. Firstly the actual boundary conditions introduced by either the sponge or duxseal are unknown. This uncertainty may become critical if the tests are to be modelled analytically or numerically. Secondly, the sponge and the duxseal material only reduce the wave reflection from the artificial boundaries, therefore such phenomenon cannot be considered completely absent.

8.4.3   Rigid Container with Hinged End-Walls

Figure 8.13 shows a schematic diagram of a rigid container with hinged end-walls. In such a design, the end-walls are permitted to rotate about the base due to the hinged connection. In order to have unison movement, the two end-walls may be connected together by a tie-rod. An example of this type of container can be found in Fishman et al. (1995) where the walls were hinged but also had some degree of flexibility. They reported strains in the walls which permitted evaluation of lateral earth pressure.

8.4.4   Equivalent Shear Beam (ESB) Container

In this design, the stiffness of the end walls of the container is designed to match the shear stiffness of the soil contained in it (Fig. 8.14). In other words the fundamental frequency of the container and soil deposit are matched by design. It is assumed that the soil behaves as assemblage of equivalent shear beams and so are the end-walls. If this condition is satisfied, the interaction between the container and the soil may be considered negligible and the stress and strain similarities can be considered accomplished. However, the shear stiffness of the soil varies during shaking depending

Table 8.3 Example of rigid containers with flexible end-walls

| Shape	Shaking direction	L-B-H [mm]	L/H	Side-walls	End-walls	Testing	Reference
Rectangular	1-D	4,270-910-1,220	3.5	Tempered plate-glass	Hinged to the box	Shaking table	Fishman et al. (1995)
Rectangular (Fig. 8.12b)	1-D	450-240-400	1.1	Perspex	Sponge (30 and 60 mm thick at top and bottom respectively)	Shaking table	Dash (2010)
Rectangular	1-D	1,920-440-600	3.2	Acrylic plate	Sponge (50 mm thick)	Shaking table	Ha et al. (2011)
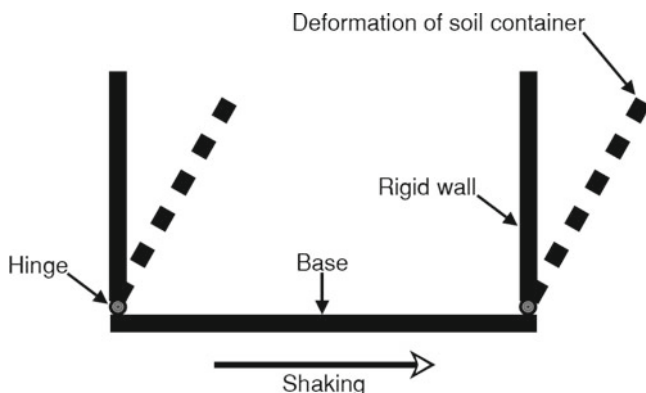
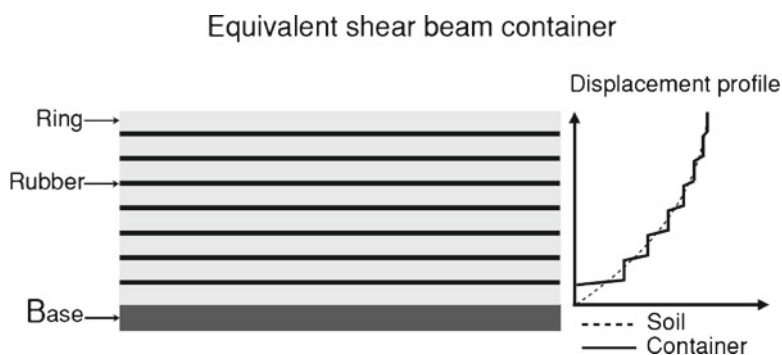**Fig. 8.13** Schematic diagram of rigid container with hinged end-walls

Fig. 8.14 Schematic diagram showing the Equivalent Shear Beam container

on the strain level. Therefore the matching of the two stiffnesses (end-wall and the soil) is possible only at a particular strain level. Schofield and Zeng (1992) explain the boundary conditions to be met by the ESB container:

1. The boundary must have the same dynamic stiffness as the adjacent soil to minimise energy reflection in the form of pressure waves.
2. The boundary must have the same friction as the adjacent soil to sustain complementary shear stresses.
3. The sidewalls should be frictionless to have plane strain condition.

   In the literature different design methods are available. The ESB box at the University of Cambridge (Zeng and Schofield 1996) was designed to match the stiffness between the container and soil over a limited range of strains in the zone of interest. On the other hand, the shear stack at the University of Bristol (Dar 1993), shown in Fig. 8.15b, is designed considering a value of strains in the soil close to the failure (0.01–1%). Therefore the Bristol container will be much more flexible than the soil deposit at lower strain amplitudes and, as a consequence, the soil will always
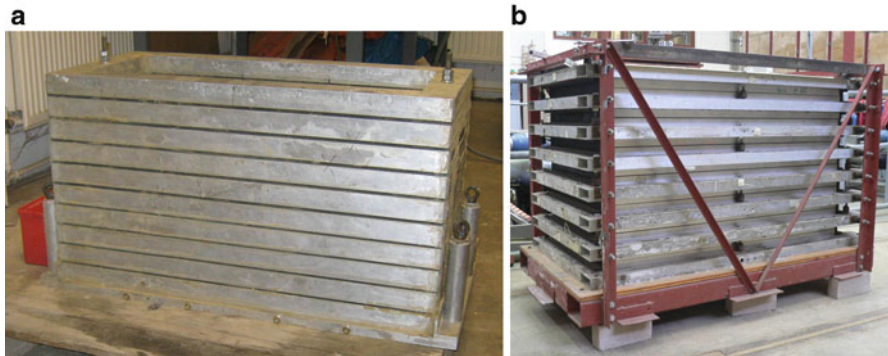
Fig. 8.15 Examples of equivalent shear beam container: (**a**) ESB used in centrifuge testing, University of Cambridge (**b**) Shear stack used in 1-g testing, University of Bristol

Table 8.4 Example of Equivalent Shear Beam container

Shape	Shaking	*L-B-H* [mm]	*L/H*	1-g/N-g	Reference
Rectangular	1-D	2,000-750-1,750	1.1	1-g	Carvalho et al. (2010)
Rectangular	1-D	1,200-550-800	1.5	1-g	Dar (1993)
Rectangular	1-D	4,270-910-1,220	3.5	1-g	Fishman et al. (1995)
Rectangular	1-D	4,800-1,000-1,200	4	1-g	Crewe et al. (1995)
Rectangular	1-D	560-250-226	2.5	N-g	Zeng and Schofield (1996)
Rectangular	1-D	800-350-600	1.3	N-g	Madabhushi et al. (1998)

dictate the overall behaviour of the container. In a recent study using the Bristol shear stack, see Bhattacharya et al. (2010), it was observed that the ratio between the container stiffness and initial stiffness of the granular deposit determined the success in reproducing the true shearing behaviour of the granular material under seismic shaking. In particular, it was observed that when a very stiff deposit was used (for example rubber granule was used to create a large stiffness contrast in a multi layered deposit), the container behaved almost like a rigid container. Under such condition, the container drives the soil shearing.

In terms of manufacturing, ESB container consists of a rectangular box made from aluminium rings separated by rubber layers. The rings provide lateral confinement of the soil in order to reproduce the K_0 conditions (zero lateral strains), while the rubber layers allowed the container to deform in a shear beam manner. Table 8.4 lists some examples of ESB container described in the literature.

8.4.4.1 Limitations

Rubber has a linear elastic stress-strain relationship up to large shear strain level. On the other hand the behaviour of the soil under cyclic loading is highly non-linear and hysteretic particularly at large strains.
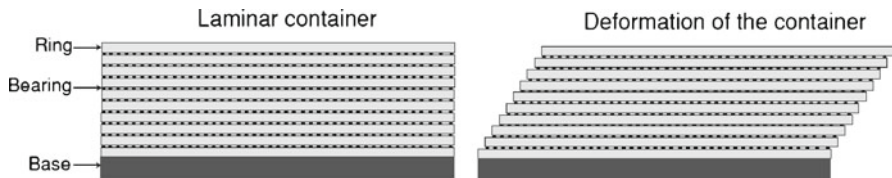
Fig. 8.16 Schematic diagram of laminar container

Table 8.5 Examples of laminar containers

Shape	Shaking	L-B-H [mm]	L/H	1-g/N-g	Design	Reference
Rectangular	1-D	900-350-470	1.9	1-g	Stack of laminae separated by bearing	Gibson (1997)
Rectangular	1-D	1,000-500-1,000	1	1-g	Stack of laminae separated by bearing	Prasad et al. (2004)
Circular	2-D	2,280-2,130 (D-H)	1.1	1-g	Container hanging on the top lamina supported by frame	Meymand (1998)
Rectangular	2-D	1,888-1,888-1,520	1.2	1-g	Laminae supported by a frame and move independently	Ueng and Chen (2010)
Rectangular	1-D	457-254-254	1.8	N-g	Stack of laminae separated by bearing	Van Laak et al. (1994)
Rectangular	1-D	710-355-355	2	N-g	Stack of laminae separated by bearing	Pamuk et al. (2007)
12-sided polygon	2-D	584-500 (D-H)	1.2	N-g	Stack of laminae separated by bearing	Shen et al. (1998)
Rectangular	1-D	900-450-807	1.1	1-g	Laminae are supported individually by bearings and steel guide connected to an external frame	Turan et al. (2009)
Square	2-D	1,000-1,000-1,000	1	1-g	Laminae are supported individually by bearings	Jafarzadeh (2004)

8.4.5 Laminar Container

Figure 8.16 shows a schematic diagram of a laminar container. The most common design consists of a stack of laminae supported individually by bearings and a steel
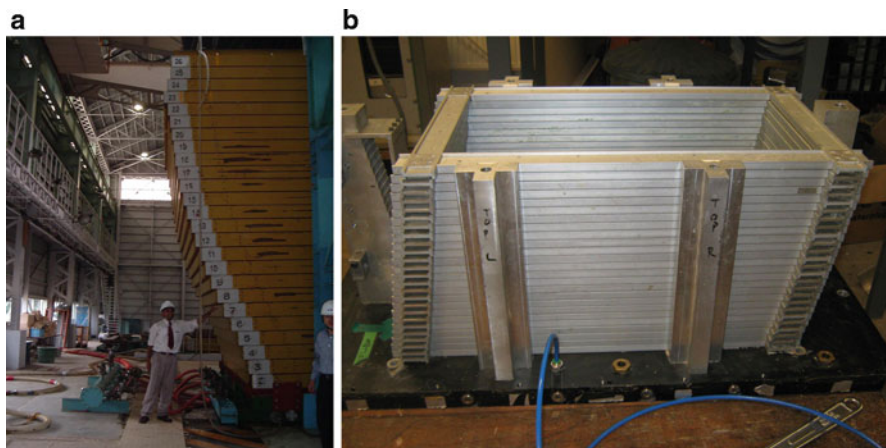
Fig. 8.17 Laminar container: (**a**) Large laminar container used in 1-g testing in Tsukuba, Japan (**b**) Laminar container used in centrifuge, University of Cambridge
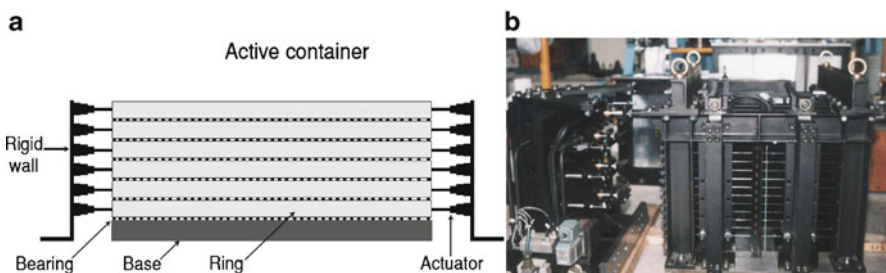

Fig. 8.18 Active boundaries container: (**a**) Schematic diagram of the container (**b**) Example of active boundaries container (Courtesy of Professor Akihiro Takahashi)

guide connected to an external frame. The design principle of a laminar box is to minimize the lateral stiffness of the container in order to ensure that the soil governs the response of the soil-box system.

Table 8.5 lists nine different types of laminar containers presented in the literature. It may be observed that most common shape is rectangular. However for two dimensional shaking tests the shape of the box can be square or circular or 12–sided polygon. Figure 8.17 shows the photograph of two laminar boxes.

8.4.6 Active Boundaries Container

The design principle of an active boundaries container is very similar to that of a laminar box with the only difference that external actuators are connected to each lamina. Different pressure may be applied from the actuator in order to achieve the desired prototype condition. This type of container may be used in a situation where

the stiffness of the soil is varying sharply during the shaking (e.g. for liquefaction application). Figure 8.18a shows the schematic diagram of an active boundary box and Fig. 8.18b shows the photograph of the active box from Tokyo Institute of Technology.

8.5 Discussion and Conclusions

There are differences between physical testing and physical modelling. Physical testing is the actual test carried out using a model (either a laboratory scale or full scale) but physical modelling refers to the modelling of a particular aspect (e.g. collapse mechanism or physical process) of a prototype problem under consideration. Physical modelling therefore requires the recognition of the physical mechanisms or processes that control the behaviour of interest and therefore the derivation of the relevant non-dimensional groups. Each physical test can be analysed as a separate prototype on its own merits. As the physical tests are real physical events, the data generated by these tests can be instructive and useful if all the variables and detailed physical parameters that contributed to the test observations are recognised. In this context, it must be mentioned that a number of distortions can be induced by the testing methods and/or artificial boundaries required to model an infinite soil medium. In this chapter, a thorough investigation on the model soil container for seismic testing of geotechnical models is considered.

Soil profile on site can never be replicated in a model and none of the physical modelling techniques are perfect. For example in 1-g testing, it is difficult to model the stress dependency behaviour of granular material. On the other hand, centrifuge testing of geotechnical models are challenging (carrying out all the actuations while the model is spinning at a high angular velocity) and the technique itself introduces errors, such as radial distortion, gravitational distortion, angular distortion, Coriolis distortion. Also, the scaled model in a centrifuge is not free of external vibrations. In this chapter, the issue of model container has been studied. The requirement of a perfect model soil container is first established from first principles. Six different types of model container designs are reviewed and discussed. Based on the review, it is realised that none of the six types of containers are suitable for all types of modelling applications. It is important to choose particular types of container depending on the problem in hand.

References

Adalier K, Elgamal AW (2002) Seismic response of adjacent saturated dense and loose sand columns. Soil Dyn Earthquake Eng 22(2):115–127

Bhattacharya S, Dihoru L, Taylor CA, Muir Wood D, Mylonakis G, Moccia F, Simonelli AL (2010) Kinematic bending moments in piles: an experimental study. In: Proceedings of the

7th international conference on urban earthquake engineering and 5th international conference on earthquake engineering, Tokyo

Bhattacharya S, Hyodo M, Goda K, Tazoh T, Taylor CA (2011a) Liquefaction of soil in the Tokyo bay area from the 2011 Tohoku (Japan) earthquake, Soil Dyn Earthquake Eng, doi:10.1016/j.soildyn.2011.06.006

Bhattacharya S, Lombardi D, Muir Wood D (2011b) Similitude relationships for physical modelling of offshore wind turbines. Int J Phys Model Geotech 11(2):58–68

Bolton MD (1986) The strength and dilatancy of sands, Géotechnique 36(1):65–78

Brennan AJ (2003) Vertical drains as a countermeasure to earthquake-induced soil liquefaction. PhD thesis, University of Cambridge

Carvalho AT, Bile Serra J, Oliveira F, Morais P, Ribeiro AR, Santos Pereira C (2010) Design of experimental setup for 1 g seismic load tests on anchored retaining walls. In: Springman S, Laue J, Seward L (eds) Physical modelling in geotechnics. Taylor and Francis Group, London

Cheney JA, Hor OYZ, Brown RK, Dhat NR (1988) Foundation vibration in centrifuge models. In: Proceedings of the Centrifuge 88, international conference on centrifuge modelling, Paris

Crewe AJ, Lings ML, Taylor CA, Yeung AK, Andrighetto R (1995) Development of a large flexible shear stack for testing dry sand and simple direct foundations on a shaking table. In: Elnashai (ed) European seismic design practice. Balkema, Rotterdam

Dar AR (1993) Development of flexible shear-stack for shaking table of geotechnical problems. PhD thesis, University of Bristol, Bristol

Dash SR (2010) Lateral pile-liquefied soil interaction during earthquakes. DPhil thesis, University of Oxford, Oxford

Fishman KL, Mander JB, Richards R Jr (1995) Laboratory study of seismic free-field response of sand. Soil Dyn Earthquake Eng 14:33–43

Gibson AD (1997) Physical scale modelling of geotechnical structures at one-g. PhD thesis, California Institute of Technology, Pasadena

Ha I, Olson SM, Seo M, Kim M (2011) Evaluation of liquefaction resistance using shaking table tests. Soil Dyn Earthquake Eng 31:682–691

Iai S (1989) Similitude for shaking table test on soil-structure-fluid model in 1 g gravitational field. Soil Found 29(1):105–118

Jafarzadeh B (2004) Design and evaluation concepts of laminar shear box for 1G shaking table tests. In: Proceedings of the 13th world conference on earthquake engineering, Vancouver, paper no. 1391

Kelly RB, Houlsby GT, Byrne BW (2006) A comparison of field and lab tests of caisson foundation in sand and clay. Géotechnique 56(9):617–626

Kramer SL (1996) Geotechnical earthquake engineering. Prentice Hall, Upper Saddle River

Leblanc C, Byrne BW, Houlsby GT (2010) Response of stiff piles to random two-way lateral loading. Géotechnique 60(9):715–721

Madabhushi SPG, Butler G, Schofield AN (1998) Design of an Equivalent Shear Beam (ESB) container for use on the US Army. In: Kimura, Takemura (eds) Centrifuge. Balkema, Rotterdam

Meymand PJ (1998) Shaking table scale model tests of nonlinear soil-pile-superstructure interaction in soft clay. PhD thesis, University of Berkley, Berkley

Muir Wood D, Crewe AJ, Taylor CA (2002) Shaking table testing of geotechnical models. Int J Phys Model Geotech 2:1–13

Ng CWW, Li XS, Van Laak PA, Hou DYJ (2004) Centrifuge modelling of loose fill embankment subjected to uni-axial and bi-axial earthquakes. Soil Dyn Earthquake Eng 24:305–318

Norton H (2008) Investigation into pile foundations in seismically liquefiable soils. MSc thesis, University of Oxford

Pamuk A, Gallagher PM, Zimmie TF (2007) Remediation of piled foundations against lateral spreading by passive site stabilization technique. Soil Dyn Earthq Eng 27:864–874

Prasad SK, Towhata I, Chandradhara GP, Nanjundaswamy P (2004) Shaking table tests in earthquake geotechnical engineering. Curr Sci 87(10):1398–1404

Schofield AN (1980) Cambridge centrifuge operations, twentieth rankine lecture. Géotechnique 30: 227–268

Schofield AN (1981) Dynamic and earthquake geotechnical centrifuge modelling. Proceedings international conference recent advances in geotechnical earthquake engineering and soil dynamics, vol 3, 1081–1100

Shen CK, Li XS, Ng CWW, Van Laak PA, Kutter BL, Cappel K (1998) Development of a geotechnical centrifuge in Hong Kong. In: Centrifuge 98(1), Tokyo

Steedman RS, Madabhushi SPG (1991) Wave propagation in sands. In: Proceedings of the international conference on seismic zonation, Stanford University, California

Turan A, Hinchberger SD, El Naggar H (2009) Design and commissioning of a laminar soil container for use on small shaking table. Soil Dyn Earthquake Eng 29:404–414

Ueng TS, Chen CH (2010) Liquefaction of sand under multidirectional shaking table test. In: Proceedings of the international conference on physical modelling in geotechnics, ICPMG, Hong Kong, pp 481–486

Van Laak P, Taboada V, Dobry R, Elgamal AW (1994) Earthquake centrifuge modelling using a laminar box. Dynamic geotechnical testing, vol 2, ASTM STP 1213. American Society for Testing and Materials, Philadelphia, pp 370–384

Whitman RV, Lambe PC (1986) Effect of boundary conditions upon centrifuge experiments using ground motion simulation. Geotech Test J 9(2):61–71

Wroth CP, Randolph MF, Houlsby GT, Fahey M (1979) A review of the engineering properties of soils with particular reference to the shear modulus. Report CUED/D-SOILS TR75, University of Cambridge

Zeng X, Schofield AN (1996) Design and performance of an equivalent-shear-beam container for earthquake centrifuge modelling. Geotechnique 46(1):83–102